Ocean Dynamics (2011) 61:403–410
DOI 10.1007/s10236-010-0335-x

Tide-induced vertical suspended sediment concentration profiles: phase lag and amplitude attenuation

Qian Yu · Burg W. Flemming · Shu Gao

Received: 24 April 2010 / Accepted: 25 August 2010 / Published online: 15 September 2010

Abstract In tidal environments, the response of suspended sediment concentration (SSC) to the current velocity is not instantaneous, the SSC lagging behind the velocity (phase lag), and the amplitude of SSC variation decreasing with height above the bed (amplitude attenuation). In order to quantitatively describe this phenomenon, a one-dimensional vertical advection–diffusion equation of SSC is derived analytically for uniform unsteady tidal flow by defining a concentration boundary condition using a constant vertical eddy diffusivity and sediment settling velocity. The solution, in simple and straightforward terms, shows that the vertical phase lag increases linearly with the height above the bed, while the amplitude of the SSC variation decreases exponentially with the height. The relationship between the SSC and the normalized current velocity can be represented by an ellipse or a line, depending on the phase lag. The lag of sediment movement or "diffusion/settling lag" is the mechanism generating the phase lag effect. Field observations used for validation show that the theoretically predicted and the observed curves of the vertical SSC phase lag and amplitude attenuation show reasonable agreement. The procedure proposed in this paper substantially simplifies the modeling of suspended matter transport in tidal flows.

Responsible Editor: Jörg-Olaf Wolff

Q. Yu (✉) · B. W. Flemming
Senckenberg Institute,
Wilhelmshaven, Germany
e-mail: qianyu.nju@gmail.com

S. Gao
MOE Laboratory for Coast and Island Development,
Nanjing University,
Nanjing, China

Keywords Suspended sediment concentration · Tidal environments · Phase lag · Amplitude attenuation · Diffusion/settling lag

1 Introduction

Tidal systems have, amongst others, been investigated with respect to their suspended sediment dynamics and budgets because these play important roles in morphologic change, contaminant transport, and biogeochemical processes. From field observations, it has long been known that, in tidal environments, the response of suspended sediment concentration (SSC) to the current velocity, or the bed shear stress, is not instantaneous, and that there is a phase lag of the SSC behind the velocity (for a summary of observations before the 1970s cf. Allen (1974)). These observations have confirmed that the lag increases with height above the seabed (Joseph 1954; Ellis et al. 2004; Souza et al. 2004). For example, measurements in the southern North Sea off the isle of Texel (Joseph 1954) recorded time lags of between 0 (near the bottom) and 3 h (near the surface). On the other hand, this phase lag effect can be represented as a "hysteresis loop" by plotting SSC time-series measurements against current velocity (Davies 1977; Kostaschuk et al. 1989; West and Sangodoyinb 1991; Whitehouse 1995; van der Ham and Winterwerp 2001; van de Kreeke and Hibma 2005; Murphy and Voulgaris 2006). At the same velocities, SSCs are usually higher in decelerating currents than in accelerating currents, this being represented by an anticlockwise loop. However, as demonstrated by Schubel (1968) and Souza et al. (2004), not only the phase difference but also the amplitude of the SSC variation decreases with height above the bed. In the present contribution, we call the decreasing amplitude in SSC the

"amplitude attenuation", in analogy to the definition of the gradual loss in the intensity of propagating signals in physics.

The quantitative interpretation of the phase lag of SSC behind velocity, and the amplitude attenuation of SSC variation, is based on the evolution of vertical SSC profiles. These represent a balance between upward turbulent diffusion and downward settling of sediment particles. Because in uniform and steady flow conditions the duration of these two processes can be estimated by h^2/K_s and h/W_s, respectively, the relative importance of these two discrete processes of dispersion and settlement can be scaled by $W_s h/K_s$, including the sediment vertical eddy diffusivity K_s and the sediment settling velocity W_s, and also the water depth h (Prandle 1997). The classic formulation introduced by Rouse (1937) for uniform and steady flow conditions is:

$$\frac{C_z}{C_a} = \left(\frac{h-z}{z}\frac{a}{h-a}\right)^{W_s/\beta\kappa u_*} \tag{1}$$

where C_z is the SSC at height z relative to that of C_a at the reference height a.

However, in the case of reversing unsteady tidal flows, the application of the Rouse formulation is questionable. Because of their inherent complexity, tidal SSC profiles are generally estimated using a variety of numerical approaches (e.g., Wang et al. 2005; Stanev et al. 2007; van der Molen et al. 2009). In some cases, analytical solutions for uniform unsteady flows were achieved by using advanced mathematical tools (Davies 1977; Smith 1977; Lavelle et al. 1984; Prandle 1997; Jung et al. 2004), but these are relatively complex and hence difficult to implement in practice.

With the development of new field observation instrumentation, especially the application of ADCPs (acoustic Doppler current and back-scatter profilers), the continuous measurement of vertical SSC profiles has become the state of the art (e.g., Holdaway et al. 1999; Souza et al. 2004). As a consequence, excellent SSC data are today available for the investigation of phase lag and the amplitude attenuation phenomena in coastal SSC profiles. However, several key parameters, e.g., the sediment settling velocity and the amplitude calibration from the ADCP back-scatter to real SSC, are still uncertain (e.g., Bartholomä et al. 2009).

In the present paper, tide-induced vertical SSC profiles were derived analytically for uniform unsteady flow by defining a concentration boundary condition (Dirichlet boundary condition; cf. Sanford and Halka 1993) in order to obtain a simpler and more straightforward solution and to allow the phase lag and amplitude attenuation to be quantitatively expressed in simple formulae. After validating the results on the basis of the data of Souza et al. (2004), the mechanism, limitations and applications of the derived solution are discussed.

2 Analytical solution

The mathematical expression of the one-dimensional vertical ($1D_V$) sediment advection-diffusivity model is:

$$\frac{\partial C}{\partial t} = W_s\frac{\partial C}{\partial z} + K_s\frac{\partial^2 C}{\partial z^2} \tag{2}$$

where C is the SSC, which is a function of the time (t) and the distance above the seabed (z), and W_s and K_s are sediment settling velocity and sediment vertical eddy diffusivity, respectively. For the sake of simplicity, K_s is assumed to be constant over time and space in tidal environments (Prandle 1997; Jung et al. 2004).

The standard practice in research on non-cohesive suspended sediment transport is to specify a bottom concentration boundary condition (a reference concentration) for Eq. 2 (Dyer 1986). This boundary condition (z=0) is here defined as an arbitrary function of time $f(t)$, which, if it converges, can be transformed to a summation of a trigonometric Fourier series:

$$C(0,t) = f(t) = N_0 + \sum_{i=1} N_i\cos(\omega_i t + \phi_i) \quad \omega_i \neq 0 \tag{3}$$

The analytical solution of Eq. 2 using the boundary condition defined in Eq. 3 can then be obtained from:

$$\begin{aligned} C(z,t) &= N_0\exp\left(-\frac{W_s}{K_s}z\right) \\ &\quad + \sum_{i=1} N_i\exp\left(-a_i\frac{W_s}{K_s}z\right)\cos\left(\omega_i t + \phi_i - b_i\frac{W_s}{K_s}z\right) \\ a_i &= \left(1+\sqrt{1+4{b_i}^2}\right)/2 \\ b_i &= \left(\frac{1+\sqrt{1+16\omega_i^2K_s^2/W_s^4}}{8}\right)^{0.5} \end{aligned} \tag{4}$$

In Eq. 4, if $4\omega_i K_s/W_s^2 \gg 1$ or $\ll 1$, coefficients a_i and b_i will reduce to:

$$\begin{aligned} &\text{Condition (A): } a_i = 0.5 + b_i = 0.5 + \frac{1}{W_s}\sqrt{\frac{\omega_i K_s}{2}} \\ &\qquad b_i = \frac{1}{W_s}\sqrt{\frac{\omega_i K_s}{2}} \text{ if } \frac{4\omega_i K_s}{W_s^2} \gg 1 \\ &\text{Condition (B): } a_i = \frac{1}{2}\left(1+\sqrt{2}\right) = 1.207 \\ &\qquad b_i = 0.5 \quad \text{if } \frac{4\omega_i K_s}{W_s^2} \ll 1 \end{aligned} \tag{5}$$

The reference concentration can be calculated in terms of the bed concentration C_0 and the normalized excess shear stress s (Smith and Mclean 1977) as:

$$\begin{aligned} C(0,t) &= C_0\gamma s/(1+\gamma s) \\ s &= (\tau-\tau_{cr})/\tau_{cr} \end{aligned} \tag{6}$$

where τ and τ_{cr} are the shear stress and critical shear stress, respectively, and γ is an empirical constant with the range of 10^{-3}~10^{-5} (Smith and McLean 1977; Hill et al. 1988; Drake and Cacchione 1989). By transforming Eq. 6 to the format of Eq. 3, the temporal and spatial evolution of SSC can be resolved by Eq. 4. This would be a general solution for arbitrary parameters.

In a simple case with a low value of (γs), Eq. 6 reduces to $C(0,\ t)=C_0\gamma s$. The shear stress, $\tau=\rho C_D\ u^2$, can be determined using the vertical mean velocity u with a constant drag coefficient C_D, and if τ is sufficiently larger than τ_{cr}, Eq. 6 can be reduced to $C(0,\ t)=\beta C_0\ \gamma\rho C_D\ u^2/\tau_{cr}$ as a first order harmonic approximation with a constant β which is less than 1. For a simple M_2 tidal current, u is assumed to be:

$$u = U\cos\omega t \tag{7}$$

where U is tidal current amplitude, and ω is the semi-diurnal constituent (M2).

On this basis, the boundary condition can finally be simplified to:

$$\begin{aligned} C(0,t) &= \frac{\beta C_0\gamma C_D U^2}{2\tau_{cr}}(1+\cos 2\omega t) = N(1+\cos 2\omega t) \\ N &= \frac{\beta C_0\gamma C_D U^2}{2\tau_{cr}} \end{aligned} \tag{8}$$

where the solution of C(z, t) can be easily obtained using Eq. 4:

$$\begin{aligned} C(z,t) &= N\exp\left(-\frac{W_s}{K_s}z\right)+ \\ &\quad N\exp\left(-a\frac{W_s}{K_s}z\right)\cos\left(2\omega t - b\frac{W_s}{K_s}z\right) \\ a &= \left(1+\sqrt{1+4b^2}\right)/2 \\ b &= \left(\frac{1+\sqrt{1+64\omega^2K_s^2/W_s^4}}{8}\right)^{0.5} \end{aligned} \tag{9}$$

Equation 9 shows that the SSC profile has a time-independent, exponentially decreasing term (the first term of RHS of Eq. 9) and an M4 quarter-diurnal variation term (the second term of RHS of Eq. 9). The time-independent, exponentially decreasing term equals the SSC profile when the averaged reference boundary concentration ($C(0,\ t)=N$) is in steady state. This term represents the time averaged SSC profile.

For the quarter-diurnal variation term, the vertical phase lag and the amplitude attenuation are given by:

$$\varphi(z) = b\frac{W_s}{K_s}z \tag{10}$$

$$A(z) = N\exp\left(-a\frac{W_s}{K_s}z\right) \tag{11}$$

where $\varphi(z)$ is the vertical phase lag, and $A(z)$ is the vertical amplitude attenuation of the periodic variation term. Equation 10 demonstrates that the vertical phase lag increases linearly with the height above the bed, and Eq. 11 demonstrates that the amplitude decreases exponentially with the height above the bed, both being controlled by the tidal frequency ω, the settling velocity W_s, and the vertical sediment eddy diffusivity K_s. In this formulation a is always larger than 1, which indicates that the amplitude attenuation of the SSC variation is faster than the rate of decrease of the time averaged SSC, as can be seen by comparing Eq. 11 with the first term of RHS of Eq. 9.

In accordance with Eq. 5, in Condition (A) associated with a large $8\omega K_s/W_s^2$, the sediment is relatively fine, and the eddy diffusivity is relatively strong, then Eqs. 10 and 11 reduce to:

$$\varphi(z) = \sqrt{\frac{\omega}{K_s}}z \tag{12}$$

$$A(z) = N\exp\left[-\left(\frac{W_s}{2K_s}+\sqrt{\frac{\omega}{K_s}}\right)z\right] \tag{13}$$

Equation 12 shows that, in the case of a strong eddy diffusivity and fine-grained sediments, the rate of phase lag increase is only influenced by ω and K_s, and is neither related to W_s nor to the sediment grain size. If, on the other hand, in Condition (B), the sediment is relatively coarse with a low eddy diffusivity, then a and b are both constant. This suggests that the rates of phase lag increase and amplitude decrease are only controlled by K_s and W_s, neither being related to ω. This suggests that another time scaling parameter, namely the tidal frequency ω, is of importance in addition to the basic scaling W_sh/K_s for steady and uniform flow (Prandle 1997). In Condition (B), the coarse sediment having a low eddy diffusivity causes the reduced effects in the tidal variation time scale, and as a result, the independence of the solution to ω. It is also noted that Eq. 12 of the phase lag in SSC is of the same character as the lag in turbulent kinetic energy (TKE) production in Simpson et al. (2000).

Integrating Eq. 9, the vertical averaged SSC can be written as:

$$\overline{C(t)} = \frac{1}{h}\int_0^h C(z,t)dz = \frac{N}{h}\frac{K_s}{W_s}\left\{\begin{array}{l} 1-\exp\left(-\frac{W_s}{K_s}h\right) \\ +\frac{1}{\sqrt{a^2+b^2}}\left[\cos\left(2\omega t-\tan^{-1}\frac{b}{a}\right)-\exp\left(-a\frac{W_s}{K_s}h\right)\cos\left(2\omega t-\tan^{-1}\frac{b}{a}-b\frac{W_s}{K_s}h\right)\right]\end{array}\right\} \quad (14)$$

where h is the water depth. The typical values of W_s and K_s are in the order of 10^{-2} to 10^{-3}, and the water depth in the order of 10 m. If $W_s\ h/K_s$ is sufficiently larger than 1, considering $a>1$, the terms $\exp(-W_s\ h/K_s)$ and $\exp(-aW_s\ h/K_s)$ in this equation will be much lower than 1. In this situation, we neglect these terms, and the vertically averaged SSC is:

$$\overline{C(t)} = \frac{N}{h}\frac{K_s}{W_s}\left[1+\frac{1}{\sqrt{a^2+b^2}}\left[\cos\left(2\omega t-\tan^{-1}\frac{b}{a}\right)\right]\right] \quad (15)$$

This simplified solution can provide a clear estimation of the phase lag of the vertically averaged SSC behind the velocity, which is $\tan^{-1}$(b/a) and ranges between 0 and 0.5π. It should be noted that this simplified solution is only valid in the conditions mentioned above. While the Neumann boundary condition (zero sediment flux at the sea surface) would be valid for a greater range of conditions, the analytical expression of the vertically averaged SSC would then be much more complex, and that would be beyond the scope of the present paper.

In Fig. 1, the predicted temporal evolution of SSC profiles are demonstrated for a representative tidal situation with W_s=2 mms^{-1}, K_s=0.02 m^{2}s^{-1}, $\omega = 1.4\times10^{-4}$ s^{-1}, and a 20 m water depth. In this case, the vertical phase lag is 5.24° per meter, and the amplitude of SSC variation is 0.86 times that at the location 1 m deeper.

The relationship between current velocity and SSC at a given height above the bed is specified in terms of Eqs. 7 and 9, which can be simply represented as the relation of function $y(t)$ and the normalized velocity $x(t)$ at a given depth:

$$y(t) = \cos(2\omega t-\varphi) \quad (16)$$

$$x(t) = \left(\frac{u}{U}\right)^2 = \frac{1}{2}(\cos 2\omega t-1) \quad (17)$$

Function $y(t)$ in Eq. 16 represents the variation of SSC, being the simple-harmonic variation term in Eq. 9, other parts in Eq. 9 all being independent of time and hence of velocity, while φ is the phase lag defined in Eq. 10. Function $x(t)$ in Eq. 17 is the square of the normalized velocity, which has the same frequency as $y(t)$ and represents the current speed (the absolute value of velocity). This relationship is similar to the phase difference model suggested by Allen (1974). It is easy to eliminate the time between Eqs. 16 and 17, and to transform the relationship between y and x to a standard ellipse function:

$$\begin{array}{l}(1-\cos\varphi)X^2+(1+\cos\varphi)Y^2=(\sin\varphi)^2 \\ X=(2x+y-1)/\sqrt{2} \\ Y=(y-2x+1)/\sqrt{2}\end{array} \quad (18)$$

When $\varphi=k\pi$ (k=0, 1, 2...), Eq. 18 mathematically transforms into a line, which demonstrates that there are unique SSCs corresponding to given current speeds. If $\varphi\neq k\pi$, this equation describes an elliptical loop, the lengths of the major and minor axes of which are controlled by the phase lag φ. This indicates that, for a given current speed, there are two corresponding SSCs, one being associated with the accelerating, the other with the decelerating current speed. These elliptical loops are illustrated with respect to different values of φ=0, $\pi/4$, $\pi/2$ and $3/4\pi$ in Fig 2.

Because the phase lag φ increases linearly with the height (z) in terms of Eq. 10, the relationships between speed and SSC change with z. In the near-bed area, where most observations of SSC are made (e.g., Cacchione et al. 2006), a low phase lag φ (usually between 0 and 0.5π) produces counterclockwise loops in this relationship. A characteristic feature is that during accelerating flow the SSC is lower than during decelerating flow at corresponding current speeds, similar to the ellipse in Fig. 2 where $\varphi=\pi/4$. This is consistent with the general pattern of the observations cited in the introduction. In accordance with a phase lag of $\tan^{-1}$(b/a) in Eq. 15, which ranges between 0 and 0.5π, the depth-averaged SSC has a similar relationship with current speed.

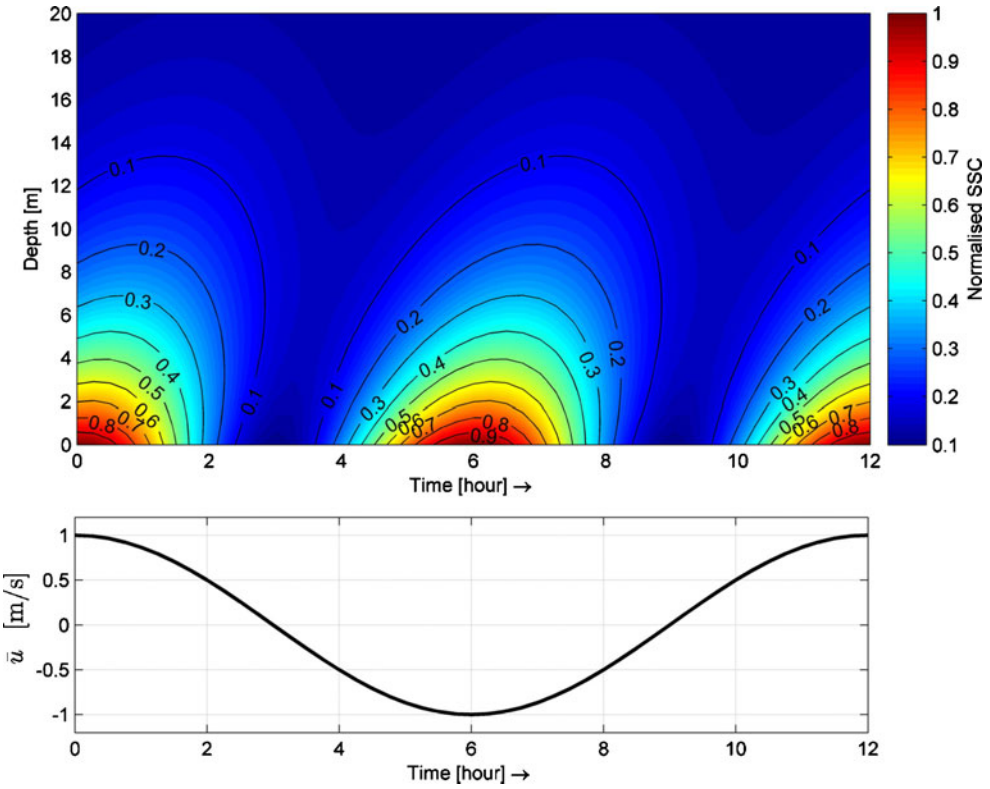

Fig. 1 Prediction of the variation in SSC with time in an M_2 tidal cycle. The predicted SSCs are calculated by Eq. 9 for a representative tidal situation with W_s=2 mms^{-1}, K_s=0.02 m^{2}s^{-1}, $\omega = 1.4 \times 10^{-4}$ s^{-1}, at a 20-m water depth. The SSC is normalized by the maximum value

3 Validation

To validate our analytical solution of the vertical SSC phase lag and amplitude attenuation, the observations of Souza et al. (2004) were utilized. These authors had deployed a 1,200 kHz acoustic Doppler current profiler (ADCP) over a spring tidal period between 27 and 29 May 2002 at a mean water depth of about 25 m in the tidally mixed region of the upper Gulf of California. The mean velocities and Reynolds stresses were estimated using two pairs of opposing acoustic beams, and the SSC was estimated from the acoustic back-scatter. During the observational period, the tides were dominated by semi-diurnal components, the tidal velocities being almost rectilinear and of the order of 0.6 ms^{-1} near the sea surface and 0.3 ms^{-1} near the bottom. The eddy viscosity and sediment settling velocity were estimated to be between 10^{-3} and 10^{-2} m^{2}s^{-1} and 0.0001 and 0.001 ms^{-1}, respectively. The vertical phase lag and the amplitude of SSC from 1 to 7 m above the seabed were also taken from Souza et al. (2004) (see Fig. 3).

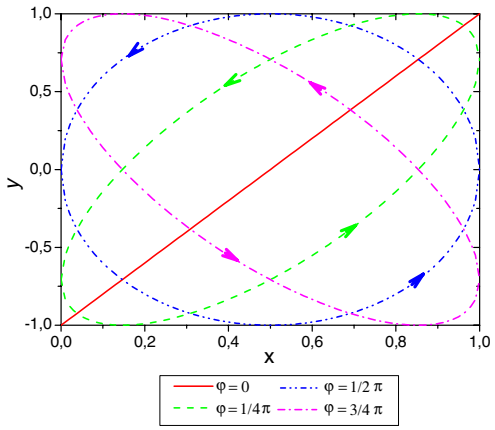

Fig. 2 Relationships between current speed and SSC at a given height above the bed where y and x are defined by Eqs. 16 and 17, respectively. y represents the variation of SSC, and x is the square of the normalized velocity representing the current speed (the absolute value of velocity). The resulting curves are either ellipses or straight lines, depending on the phase lag φ. The *arrows* indicate the direction of change in the individual curves (cf. text for details)

The analytical solution uses the observed values of W_s and K_s with an M_2 frequency of 1.4×10^{-4} s^{-1}. The eddy diffusivity is usually considered to be equal to the water eddy viscosity (Dyer 1986), K_s being chosen as 0.9×10^{-2} m^{2}s^{-1}, and the settling velocity being set at 0.00075 ms^{-1}. The theoretically predicted curves of the vertical SSC phase lag and amplitude attenuation are illustrated in Fig. 3a, b, which show reasonable agreement between observations and predictions.

From Fig. 3b, it can be seen that the analytical solution predicts the vertical phase lag better than the amplitude attenuation, the most pronounced departure between the predicted and observed amplitude attenuation curves being located in the intense attenuation region of the lower part of the profile. This phenomenon can be explained by the effect of the sediment grain-size spectrum at the ADCP site.

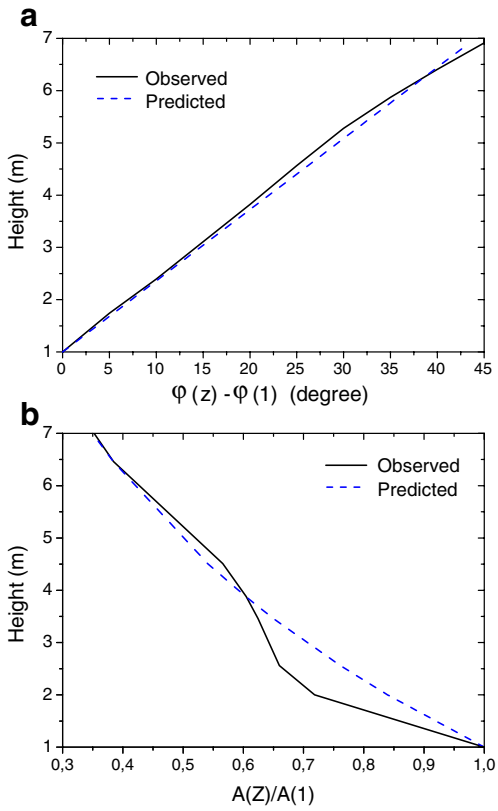

Fig. 3 **a** The vertical SSC phase lag from 1 to 7 m above the bed (the values are relative to the bottom phase). **b** The vertical SSC amplitude attenuation from 1 to 7 m above the bed (the values are normalized to the bottom amplitude). The observed curves are from Souza et al. (2004), the predicted curves based on Eqs. 10 and 11, respectively

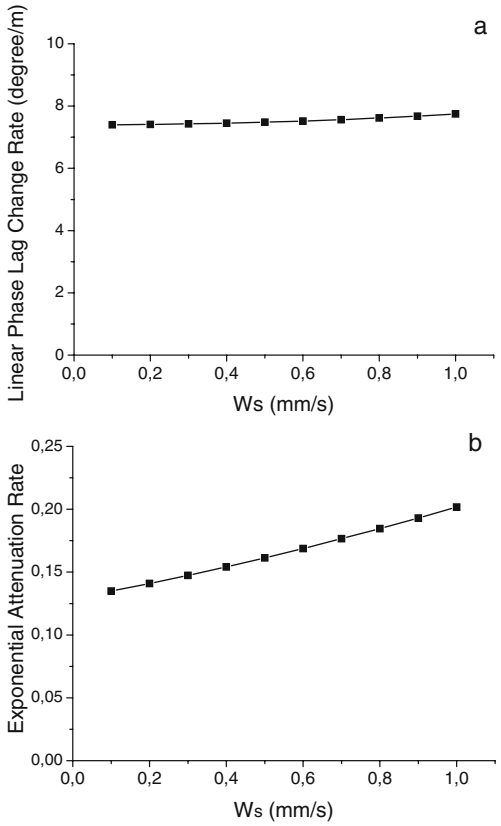

Fig. 4 **a** The relationship between the rate of linear phase lag change (bW_s/K_s, see Eq. 10) and particle settling velocity. **b** The relationship between the rate of exponential amplitude attenuation (aW_s/K_s, see Eq. 11) and particle settling velocity. Both datasets were calculated using Eq. 9 with $K_s = 0.9 \times 10^{-2}$ m^2 s^{-1} and $\omega = 1.4 \times 10^{-4}$ s^{-1}

If $K_s = 0.9 \times 10^{-2}$ m^2 s^{-1} and $\omega = 1.4 \times 10^{-4}$ s^{-1} then, based on the W_s range of 0.0001 and 0.001 ms^{-1}, $8\omega K_s/W_s^2$ will change from 10^3 to 10, which is still sufficiently larger than 1. In terms of the analysis of Eqs. 12 and 13, the rate of phase lag change is almost unrelated to W_s, but the exponential rate on amplitude attenuation is strongly influenced by W_s (see Fig. 4). This indicates that the mixture of different grain sizes has little effect on the rate of phase lag change but a significant effect on the rate of amplitude attenuation.

Due to the presence of coarse grains with relatively large settling velocities, the total SSC amplitude tends to decrease more rapidly, as shown in the lower part of Fig. 3b where the height above the bed is less than 2.5 m. Because of the rapid attenuation of coarse grains with distance from the bed, their contribution to the total SSC amplitude diminishes rapidly and can eventually be neglected when the distance to the bed is large enough. In the part of the profile away from the bed, most of the suspended sediment is composed of fine grains associated with lower attenuation rates (see Fig. 4b). That is why the amplitude attenuation rate is reduced in the upper part of Fig 3b. It should be noted that the theoretically predicted curve in Fig. 3 can be considered to represent an average relationship.

4 Discussion

The mechanism generating the phase lag effect demonstrated above is the lag of sediment movement or the "diffusion/settling lag". The concept of "settling lag", which was originally proposed by van Straaten and Kuenen (1958) and Postma (1961) to explain the net landward directed sediment transport on tidal flats, is related to the time needed for the sediment to settle out during decreasing flow. In analogy, the "diffusion lag" is associated with the time needed for the sediment to be transported from a high concentration level to a low concentration level by the diffusion process. Diffusion lag can both act during accelerating and decelerating flows when SSC gradients exist. In a period of accelerating flow, bottom SSC increases rapidly with increasing current speed, which causes an upward decreasing SSC, the sediment needing time to be lifted to a higher level by the upward diffusion

process. In a period of decelerating flow, bottom SSC decreases rapidly with decreasing current speed, which causes a downward decreasing SSC, the sediment needing time to be transported from a higher level to a lower level by the downward diffusion process. The settlement of sediment compensates the upward diffusion and enhances the downward diffusion. Because it takes more time for sediment to be lifted/settle to/from a higher level, the phase lag increases with distance above the bed, as predicted by Eq. 10. In short, the phase lag is the time taken for sediment to respond to the changing current.

Being controlled by two opposing processes, the influence of sediment settling velocity on the response of SSC to the periodic currents is complex. The high settling velocity of coarse grains hinders the upward movement of sediment by diffusion when the velocity increases. This results in a delayed response of SSC and a large phase lag, but it also enhances rapid downward settling in response to the decreasing velocity, which is associated with a small phase lag. Substituting the expression of parameters a and b in Eq. 9 into Eq. 10, it can be seen that the phase lag at a given height above the bed correlates positively with the settling velocity, implying a stronger contribution of the former process. However, in terms of Eq. 15, the phase lag of the vertically averaged SSC ($\tan^{-1}(b/a)$) correlates inversely with the settling velocity, suggesting the importance of the latter process. This apparent contradiction can be explained by the rapid amplitude attenuation of coarse grains. Although coarse grains have a larger phase lag at a given height, the amplitude of the variation of fine grains is larger than that of coarse grains, which indicates that the number of delayed coarse grains is smaller than that of fine grains, and hence the vertically integrated and averaged SSC has a larger phase lag with fine grains.

Several other factors, which are not included in the present solution, may also be involved in producing the phase lag effect. One contribution is the phase lag of the turbulent Reynolds stresses and the kinetic energy behind the velocity (Allen 1974; Dyer 1986), which has been observed in tidal environments by Gordon (1975) and Thwaites and Williams (2001). Since the turbulence intensity influences sediment eddy diffusivity, the phase lag of turbulence intensity automatically causes a phase lag in SSC. Another factor involved in the phase lag is the contribution of "scour lag" (Allen 1974), which denotes the difference between the critical sediment erosion velocity and the deposition velocity (Postma 1961), but this is of less importance in the case of non-cohesive sediments. In addition, SSC profiles and their response to velocity are distorted by the influence of non-uniform horizontal sediment concentrations (Bass et al. 2002), limitations in sediment availability on the bed, the so-called bed armoring effect (Velegrakis et al. 1997), and stratification effects induced by salinity and/or sediment (Hamblin 1989; Wang et al. 2005).

In the solution, a constant vertical sediment eddy diffusivity K_s is assumed over time and space, in correspondence to several previous analytical approaches (Prandle 1997; Jung et al. 2004). However, as shown by Souza et al. (2004), in the tidal environments K_s will change greatly both in time and in the vertical domain. The potential effects of such inconstant K_s are currently still difficult to quantify analytically, but should clearly be investigated in future studies. It is suspected that, because sediment erosion, diffusion and high SSC peaks are strongly associated with high velocities, the harmonic signals of SSC variations are possibly more related to such high-velocity conditions. As a result, the constant K_s fitted to SSC observations may be close to the observed peak K_s values in M2 tidal flows. This consideration is consistent with fact that the K_s value of 0.9×10^{-2} m^2s^{-1} used in Fig. 3 for validation is close to the peak K_s value of about 10^{-2} m^2s^{-1} observed by Souza et al. (2004). In addition, Souza et al. (2004) applied the analytical solution of Simpson et al. (2000) in the vertical phase lag of TKE production with a constant vertical eddy viscosity (equal to K_s (Dyer 1986)), the result satisfying the eddy viscosity at a value of about 10^{-2}, which is also in good agreement with the observed peak K_s values.

There are several applications of the analytical solution presented here. Firstly, when the classic Rouse equation is used for fitting SSC profiles from which the Rouse number is then derived (e. g., Amos et al. 2010), it is tacitly assumed that sediment diffusion and settling take place rapidly enough to attain steady Rouse profiles. The analytical solution, however, shows that this assumption can cause systematic errors, i.e., the Rouse number may be overestimated for accelerating flows, and underestimated for decelerating flows because of the phase lag effect. As a result, care must be taken when using the Rouse equation if phase lag effects are significant.

Another application is that the phase lag effect has a potential influence on sediment transport and hence morphodynamic modeling. Since the SSC is higher in decelerating than in accelerating flows, the suspended sediment transport rate is higher in decelerating flows, and this contributes to the residual sediment transport if the tidal current is asymmetrical (Groen 1967; Hoitink et al. 2003). Finally, it should be noted that there is a complicated relationship between concentration or suspended sediment transport rate and current speed, and that, as a consequence, the chronology of a sediment transport situation needs to be taken into consideration.

5 Conclusions

The analytical solution for generating tide-induced vertical SSC profiles presented in this paper produces simple patterns and trends, which show that the vertical phase lag of SSC

behind velocity increases linearly with the height above the bed, and that the amplitude of SSC variations decreases exponentially with the height, both being controlled by the tidal frequency, the particle settling velocity, and the vertical sediment eddy diffusivity. The relationship between SSC and normalized current velocity can be described by an ellipse or a line with respect to different phase lags.

Acknowledgements During the study, QY was supported by the Senckenberg Institute, the Chinese Scholarship Committee (CSC), the Natural Science Foundation of China (NSFC, grant number 40876043) and the Bremen International Graduate School for Marine Sciences (GLOMAR). SG was supported by the Natural Science Foundation of China (NSFC, grant number 40830853). The constructive comments of three anonymous reviewers have substantially contributed to improving the clarity of the manuscript.

References

Allen JRL (1974) Reaction, relaxation and lag in natural sedimentary systems: general principles, examples and lessons. Earth Sci Rev 10:263–342

Amos CL, Villatoro M, Helsby R, Thompson CEL, Zaggia L, Umgiesser G, Venturini V, Are D, Sutherland TF, Mazzoldi A, Rizzetto F (2010) The measurements of sand transport in two inlets of Venice lagoon; towards understanding the estuarine budget. Estuar Coast Shelf Sci 87:225–236

Bartholomä A, Kubicki A, Badewien TH, Flemming BW (2009) Suspended sediment transport in the German Wadden Sea—seasonal variations and extreme events. Ocean Dyn 59:213–225. doi:10.1007/s10236-009-0193-6

Bass SJ, Aldridge JN, McCave IN, Vincent CE (2002) Phase relationships between fine sediment suspensions and tidal currents in coastal seas. J Geophys Res 107(C10):3146. doi:10.1029/2001JC001269

Cacchione DA, Sternberg RW, Ogston AS (2006) Bottom instrumented tripods: History, applications, and impacts. Cont Shelf Res 26:2319–2334

Davies AG (1977) A mathematical model of sediment in suspension in a uniform reversing tidal flow. Geophys J R Astron Soc 51:503–529

Drake DE, Cacchione DA (1989) Estimates of the suspended sediment reference concentration (C_a) and resuspension coefficient (γ_0) from near-bed observations on the California shelf. Cont Shelf Res 9:51–64

Dyer KR (1986) Coastal and estuarine sediment dynamics. Wiley, New York, 342

Ellis KM, Bowers DG, Jones SE (2004) A study of the temporal variability in particle size in a high-energy regime. Estuar Coast Shelf Sci 61:311–315

Gordon CM (1975) Sediment entrainment and suspension in a turbulent tidal flow. Mar Geol 18:M57–M64

Groen P (1967) On the residual transport of suspended matter by an alternating tidal current. Neth J Sea Res 3–4:564–574

Hamblin P (1989) Observations and model of sediment transport near the turbidity maximum of the upper Saint Lawrence Estuary. J Geophys Res 94(C10):14419–14428

Hill PS, Nowell ARM, Jumars PA (1988) Flume evaluation of the relationship between suspended sediment concentration and excess boundary shear stress. J Geophys Res 93:12499–12509

Hoitink AJF, Hoekstra P, van Maren DS (2003) Flow asymmetry associated with astronomical tides: Implications for the residual transport of sediment. J Geophys Res 108(C10):3315

Holdaway GP, Thorne PD, Flatt D, Jones SE, Prandle D (1999) Comparison between ADCP and transmissometer measurements of suspended sediment concentration. Cont Shelf Res 19:421–441

Joseph J (1954) Die Sinkstoffführung von Gezeitenströmen als Austauschproblem. Arch Met Geophys Bioklin (A) 7:482–501

Jung KT, Jin JY, Kang H-W, Lee HJ (2004) An analytical solution for the local suspended sediment concentration profile in tidal sea region. Estuar Coast Shelf Sci 61:657–667

Kostaschuk RA, Luternauer JL, Church MA (1989) Suspended sediment hysteresis in a salt-wedge estuary, Fraser River, Canada. Mar Geol 87:273–285

Lavelle JW, Mofjeld HO, Barker ET (1984) An in situ erosion rate for a fine-grained marine system. J Geophys Res 89(C):6543–6552

Murphy S, Voulgaris G (2006) Identifying the role of tides, rainfall and seasonality in marsh sedimentation using long-term suspended sediment concentration data. Mar Geol 227:31–50

Postma H (1961) Transport and accumulation of suspended matter in the Dutch Wadden Sea. Neth J Sea Res 1:148–190

Prandle D (1997) Tidal characteristics of suspended sediment concentrations. J Hydraul Eng 123:341–350

Rouse H (1937) Modern conceptions of the mechanics of fluid turbulence. Trans Am Soc Civ Eng 102:436–505

Sanford LP, Halka JP (1993) Assessing the paradigm of mutually exclusive erosion and deposition of mud, with examples from upper Chesapeake Bay. Mar Geol 114:37–57

Schubel JR (1968) Turbidity maximum of the northern Chesapeake Bay. Science 161:1013–1015

Simpson JH, Rippeth TP, Campbell AR (2000) The phase lag of turbulent dissipation in tidal flow. In: Yanagi T (ed) Interactions between estuaries, coastal seas and shelf seas. Terra Scientific Publishing Company, Tokyo, pp 57–67

Smith JD (1977) Modeling of sediment transport on continental shelves. In: Goldberg ED, McCave IN, O'Brien JJ, Steele JH (eds) The sea marine modeling, vol 6. Wiley, New York, pp 539–577

Smith JD, McLean SR (1977) Spatially averaged flow over a wavy surface. J Geophys Res 82:1735–1746

Souza AJ, Alvarez LG, Dickey TD (2004) Tidally induced turbulence and suspended sediment. Geophys Res Lett 31:L20309. doi:10.1029/2004GL021186

Stanev EV, Brink-Spalink G, Wolff J-O (2007) Sediment dynamics in tidally dominated environments controlled by transport and turbulence: a case study for the East Frisian Wadden Sea. J Geophys Res 112:C04018. doi:10.1029/2005JC003045

Thwaites FT, Williams AJ (2001) BASS measurements of currents, waves, stress, and turbulence in the North Sea bottom-boundary layer. IEEE J Oceanic Eng 26:161–170

van de Kreeke J, Hibma A (2005) Observations on silt and sand transport in the throat section of the Frisian Inlet. Coastal Eng 52:159–175

van der Ham R, Winterwerp JC (2001) Turbulent exchange of fine sediments in a tidal channel in the Ems/Dollard estuary. Part II. Analysis with a 1DV numerical model. Cont Shelf Res 21:1629–647

van der Molen J, Bolding K, Greenwood N, Mills DK (2009) A 1-D vertical multiple grain size model of suspended particulate matter in combined currents and waves in shelf seas. J Geophys Res 114:F01030. doi:10.1029/2008JF001150

van Straaten LMJU, Kuenen PH (1958) Tidal action as a cause of clay accumulation. J Sed Petrol 28:406–413

Velegrakis AF, Gao S, Lafite R, Dupont JP, Huault MF, Nash LA, Collins MB (1997) Resuspension and advection processes affecting suspended particulate matter concentrations in the central English Channel. J Sea Res 38:17–34

Wang XH, Byun DS, Wang XL, Cho YK (2005) Modelling tidal currents in a sediment stratified idealized estuary. Cont Shelf Res 25:655–665

West JR, Sangodoyinb AYA (1991) Depth-mean tidal current and sediment concentration relationships in three partially mixed estuaries. Estuar Coast Shelf Sci 32:141–159

Whitehouse R (1995) Observations of the boundary layer characteristics and the suspension of sand at a tidal site. Cont Shelf Res 15:1549–1567